Role of nanophotonics in the birth of seismic megastructures

Stéphane Brule, Stefan Enoch, Sebastien Guenneau

Review article

Stéphane Brûlé, Stefan Enoch and Sébastien Guenneau*

Role of nanophotonics in the birth of seismic megastructures

https://doi.org/10.1515/nanoph-2019-0106
Received April 8, 2019; revised July 6, 2019; accepted July 6, 2019

Abstract: The discovery of photonic crystals 30 years ago in conjunction with research advances in plasmonics and metamaterials, has inspired the concept of decameter scale metasurfaces, coined seismic metamaterials for an enhanced control of surface (Love and Rayleigh) and bulk (shear and pressure) elastodynamic waves. These powerful mathematical tools of coordinate transforms, effective medium and Floquet-Bloch theories which have revolutionized nanophotonics, can be translated in the language of civil engineering and geophysics. Experiments on seismic metamaterials made of buried elements in the soil demonstrate that the fore mentioned tools make a possible novel description of complex phenomena of soil-structure interaction during a seismic disturbance. But the concepts are already moving to more futuristic concepts and the same notions developed for structured soils are now used to examine the effects of buildings viewed as above surface resonators in megastructures such as metacities. But this perspective of future should not make us forget the heritage of the ancient peoples. Indeed, we finally point out the striking similarity between an invisible cloak design and the architecture of some ancient megastructures as the antique Gallo-Roman theaters and amphitheatres.

Keywords: metasurfaces; seismic metamaterials; cloaking; lensing; earthquake protection; seismic ambient noise.

***Corresponding author: Sébastien Guenneau,** Aix Marseille Univ, CNRS, Centrale Marseille, Institut Fresnel, 52 Avenue Escadrille Normandie Niemen, 13013 Marseille, France,
e-mail: sebastien.guenneau@fresnel.fr. https://orcid.org/0000-0002-5924-622X
Stéphane Brûlé and Stefan Enoch: Aix Marseille Univ, CNRS, Centrale Marseille, Institut Fresnel, 52 Avenue Escadrille Normandie Niemen, 13013 Marseille, France

1 Introduction: birth of a new era for metamaterials

One may wonder what is the link between seismic megastructures and nanophotonics, where photonics merge with nanoscience and nanotechnology, and where spatial confinement considerably modifies light propagation and light-matter interaction [1].

Seismic megastructures interact with decametric to hectometric wavelengths, while nano-optics usually refer to situations involving ultraviolet, visible, and near-infrared light i.e. free-space wavelengths ranging from 300 to 1200 nm.

As a transposition of the definition of nanophotonics, we would like to postulate that "seismic megastructures involve the science and engineering of mechanical wave-matter interactions that take place on wavelength and subwavelength scales where artificial structured matter controls the interactions". Two large scale experiments carried out in France in 2012 [2, 3] demonstrate that it is possible to start the analysis of structured soils with the specific tools of condensed matter, in particular photonic crystals (PCs) and metamaterials.

In the first large scale experiment, which took place near the French city of Grenoble in August 2012, an array of boreholes were drilled in a sedimentary soil where the Rayleigh wave velocity was first estimated to be 78 m/s, thanks to a preliminary seismic test that pointed the wave time arrival at various offsets from a rotating source at 50 Hz (a vibrating probe set on a crane). The experimental mesh was made of three discontinuous lines of ten boreholes 0.32 m in diameter. The length of columns was about 5 m and the mesh spacing was 1.73 m. Numerical simulations performed with finite elements predicted a stop-band centered around 50 Hz for elastic surface waves propagating in such a large scale phononic crystal. It was experimentally confirmed that there was 5 times less elastic energy behind the seismic metamaterial after the boreholes had been carried out, in comparison with what was measured in the absence of boreholes. This confirmed an analogy could be drawn with photonic band gaps in

optics. Moreover, the measured elastic energy was 2.3 times larger at the rotating source when it was in presence of the array of boreholes, which is also analogous to the local density of states obtained for a source placed near a mirror in optics (or a PC). These results suggested the strong potential of the large-scale periodic structure for the control of spontaneous emissions of seismic waves in a way similar to what has been achieved for light in PCs 40 years ago [4, 5], and we shall go back to this historical connection in the next section.

Although we coined this large scale phononic crystal as "seismic metamaterial", the observed physical phenomena were mostly interpreted in light of Bragg scattering phenomena, and thus we must admit the terminology used was not fully legitimate at this stage.

In the second large scale experiment, which took place near the French city of Lyon in September 2012, the large scale phononic crystal was made of five rows of self-stable boreholes 2 m in diameter with a center-to-center spacing of 7 m, see Figure 1A and B. The depth of the boreholes was 5 m. The measurement of the velocity of the pressure wave in the soil was given by a preliminary seismic test, pointing once again the first wave arrival at various offsets from the source. We measured the velocity around 600 m/s. The artificial source this time consisted of the fall of the 17 ton steel pounder from a height of about 12 m to generate clear transient vibration pulses. The typical waveform of the source in time-domain looked like a second order Ricker wavelet (or "Mexican hat wavelet"). The signal was characterized by a mean frequency value at 8.15 Hz ($\lambda_{\text{P-wave}} \sim 74$ m) with a range of frequencies going from 3 to 20 Hz ($30 < \lambda_{\text{P-wave}} < 200$ m). At 5 m from the impact, the peak ground acceleration was around 0.9 g (where $g = 9.81\ \text{m.s}^{-2}$ is the gravity of Earth) which was significant, but necessary to compensate for the strong attenuation versus distance in earth materials. Importantly, the void grid spacing (7 m) was lower than the smallest wavelength measured, and thus we could unambiguously refer to this structured soil as a "seismic metamaterial".

To capture the ground motion's field, we set 30 three-component velocimeters (v_x, v_y, v_z) with a corner frequency of 4.5 Hz (–3 dB at 4.5 Hz) electronically corrected to 1 Hz. The sensors were used simultaneously with a common time base and were densely set in a quarter of the investigation area (refer Supplementary Figure 1 in [3]). The pounder was consecutively dropped at five different places (see [3] for more information), and 7–12 times at each source location. Sensors remained fixed during the whole test and the complete field of velocity (80 m × 80 m) was obtained by means of the source symmetry and the symmetry of the array of boreholes with respect to a plane passing through the x-axis.

We checked that most of the energy of the source was converted into energetic surface waves. In time-domain, we discovered two main phenomena, illustrated in Figure 1C–E. The first one was a significant wave reflection

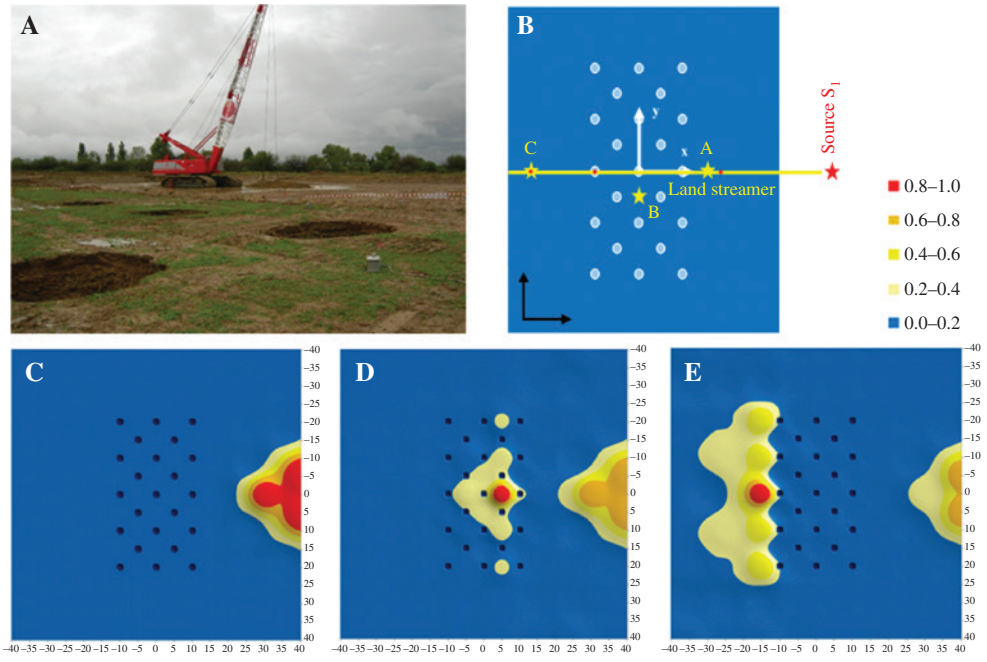

Figure 1: Experiment on a flat seismic lens: (A) Photo (courtesy of S. Brûlé) of the array of boreholes, (B), (C–E) Chronology of the x–y spatial distribution of normalized $v^2(t)$ from (C) 1.900 s to (D) 2.124 s to (E) 2.345 s.

at the contact with the long-side of the grid up to 2.1 s. The second phenomenon, illustrated in Figure 1D, was the transfer and transformation of the energy inside the grid of holes, remiscent of a first image in the Pendry-Veselago [6, 7] lens. One could finally observe a displacement of the concentration of energy inside the grid versus time along the x-axis, with a succession of transient steady-states of the maxima, which led to a focus of the signal on the other side of the grid of holes, illustrated in Figure 1E, in a way similar to what the Pendry-Veselago lens would achieve via negative refraction. Moreover, numerical simulations reveal an intimate interplay between lensing and protection with the array of boreholes, illustrated in Figure 2: a building placed on the exit of the lens is not affected by soil vibrations for a source at 12 Hz.

In our opinion, the two large scale experiments act as a foundation for a new era of metamaterials, from optics to geophysics.

However, the study of complex wave phenomena in sub-surface soils where many wave-matter interactions take place is also progressing rapidly, thanks to the development of three-dimensional surface sensors, which can be used in large numbers with good accuracy.

The spirit of data analysis has also changed a lot in the past few years. Indeed, the data processing in seismic prospection with artificial sources has been often governed by the oil and gas surface prospection approach, consisting in improving the signal to noise ratio, for a better tomography of the geological layers.

To identify the signal that contains the proofs of complex wave-matter interactions, it is necessary to modify the data acquisition and processing.

Among these geophysical techniques, we present here the on-site horizontal-to-vertical spectral ratio (HVSR) seismic method. HVSR is a non-invasive technique that can be used to estimate a dominant frequency of the soil covering the seismic substratum. Sedimentary deposits of the former Mexico lake are well-known to strongly amplify the seismic vibrations from the substratum to the free-surface of earth. In this outstanding place, we distinguish the wind- and seismic-induced horizontal vibration of a 200 m-high tower and the low-frequency vibration of the soft soils by means of HVSR. This result corroborates the idea that the city could be studied under seismic disturbance as a set of locally resonant above-surface structures and put forward the recent concept of transformational urbanism and metacity.

In this paper, we first present the main steps leading from electromagnetism to elastodynamics, thanks to correspondences in the governing equations (2), we then introduce the main features of seismic megastructures made of elastic buildings (3) and the soil-structure interaction (4). Then we extend the tool of transformation optics to seismology to design seismic cloaks (5), we further consider the

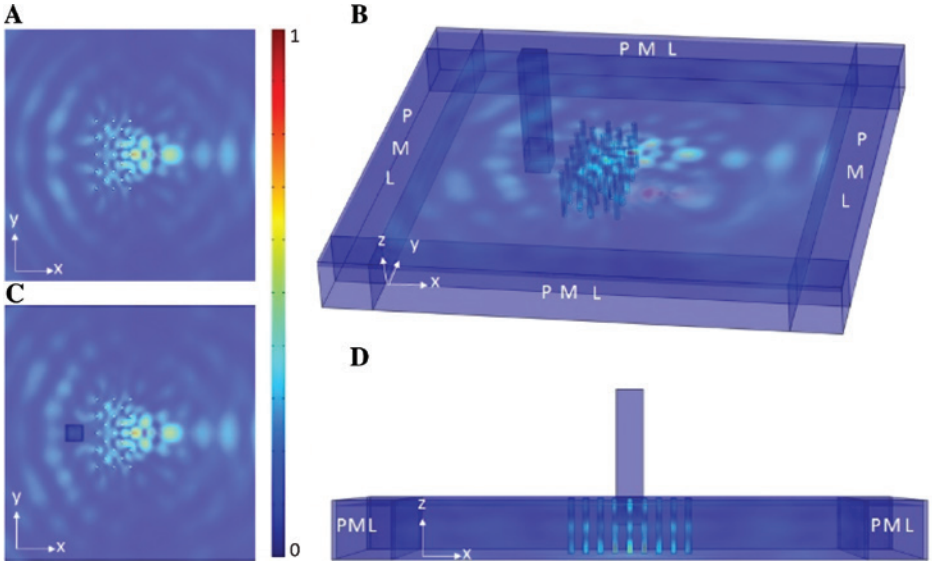

Figure 2: Finite element simulations for a plate 15 m in thickness with transverse dimensions 120 m × 120 m (including perfectly matched layers, 20 m in width) with elastic soil parameters like those in Figure 1 for a seismic source of time-harmonic frequency 12 Hz shows a shielding effect by the array (pitch 7 m) of boreholes (2 m in diameter, 15 m in depth); (A) Top view of magnitude of displacement field for boreholes on their own. Note the vanishing displacement field amplitude just behind the array of boreholes. (B) 3D view for magnitude of displacement field for boreholes with a building (similar to that in Figure 12) protected behind this array; (C) Top view of (B); (D) Side view of (B). Color scale ranges from dark blue (vanishing) to red (maximum) magnitude of displacement field and is normalized the source, to facilitate comparison with Figure 1D.

case of space folding transformations to cloak buildings outside seismic external cloaks (6), we recall the principle of seismic ambient noise measurement and apply this geophysics technique to the site of Mexico city (7), we discuss these results in light of similar phenomena arising in optics (8) and finally draw some concluding remarks with some perspectives on the future of seismic metamaterials underpinned by research advances in nanophotonics (9).

2 Correspondences between electromagnetics and elastodynamics

In 1987, the group of E. Yablonovitch and S. John reported the discovery of stop band structures for light ([4] and [5]). Photonic crystals (PCs) have, since then, found numerous applications ranging from nearly perfect mirrors for incident waves whose frequencies fall in stop bands of the PCs, to high-q cavities for PCs with structural defects [8], and waveguides with line defects.

The occurrence of stop bands in PCs also leads to anomalous dispersion whereby dispersion curves can have a negative or vanishing group velocity. Dynamic artificial anisotropy, also known as all-angle-negative-refraction [9–12], allows for focusing effects through a finite PC slab, thanks to ray trajectories according to the inverted Snell-Descartes laws of refraction, as envisioned in the 1968 paper of V. Veselago [6]. With the advent of electromagnetic metamaterials [13, 14], J. Pendry pointed out that the image through the Veselago lens can be deeply subwavelength [7], and exciting effects such as simultaneously negative phase and group velocity of light [15], invisibility cloaks [16] and tailored radiation phase pattern in epsilon near zero metamaterials were demonstrated [17] and [18]. One of the attractions of platonic crystals, which are the elastic plate analogue of photonic and phononic crystals, is that much of their physics can be translated into platonics.

To see this, let us consider a magneto-dielectric medium with a translational invariance along the z axis, in that case the propagation of transverse time-harmonic electromagnetic waves splits in two light polarizations $H(x,y,t)=(0,0,H_z(x,y))e^{i\omega t}$ and $E(x,y,t)=(0,0,E_z(x,y))e^{i\omega t}$, with ω angular wave frequency and t the time. The out-of-plane components satisfy the following two Helmholtz equations in the absence of source term:

$$\nabla\cdot(\varepsilon^{-1}\nabla H_z)+\omega^2\mu H_z=0 \tag{1}$$

$$\nabla\cdot(\mu^{-1}\nabla E_z)+\omega^2\varepsilon E_z=0 \tag{2}$$

where $\varepsilon(x,y)$ and $\mu(x,y)$ are the spatially varying electric permittivity and the magnetic permeability, and ω is the angular wave frequency.

Let us now consider an elastic plate which has small dimension along the z axis, in that case the propagation of time-harmonic flexural (Lamb) waves is modelled by displacement in the form of $U(x,y,t)=(0,0,U_z(x,y))e^{i\omega t}$, with ω angular wave frequency and t the time. The out-of-plane displacement satisfies the following Kirchhoff-Love (or biharmonic) equation in the absence of source term

$$\nabla\cdot\nabla[EI(\nabla\cdot\nabla U_z)]-\rho A\omega^2U_z=0 \tag{3}$$

where $E(x,y)$, $I(x,y)$, $A(x,y)$, $\rho(x,y)$ are the spatially varying Young's modulus, the cross-sectional moment of inertia, the cross-sectional area and the density.

One notes the strong analogy between Eq. (1–2) and Eq. (3), especially when the spatial variation of parameters is suppressed. In that case, Eq. (3) can be recast as a factor of two Helmholtz equations with a sign-shifting of the spectral parameter, what corresponds to propagating and evanescent waves that coexist in a homogeneous elastic plate, unlike for a homogeneous electromagnetic medium within which only propagating waves can exist (except in the case of medium with simultaneously negative permittivity and permeability).

There are technicalities in the mathematical analysis, and numerical modelling of the scattering of flexural waves [19] in elastic plates owing to the fourth-order partial derivatives present in the plate Eq. (3), versus the usual second-order partial derivatives for the wave Eq. (1)–(2) of optics; even waves propagating inside a perfect plate display, marked differences compared to the electromagnetic waves as the former are not dispersionless, unlike the latter. Nonetheless, drawing parallels between platonics and photonics can be used as a guidance in the design of seismic metamaterials, as these bold parallels help achieve similar effects to those observed in electromagnetic metamaterials. Notably, dynamic effects reminiscent of the time dependent subwavelength resolution observed for a flexural wave passing through a platonic flat lens consisting of 104 boreholes of 1.2 cm in diameter, drilled in a 2 mm thick duraluminium plate with transverse dimensions 30 cm × 50 cm around a frequency of 10 kHz [20] have been observed in the seismic flat lens [3]. Although, further experimental evidence is required before arriving at hasty conclusions; this suggests the possible existence of edge waves at the interface of the seismic flat lens, bearing in mind that 10 years ago subwavelength focusing properties [21] of acoustic waves

via negative refraction have been achieved, thanks to plasmon-like modes at the interfaces of a slab PC lens.

Actually, a visionary research paper on phononic crystals provided numerical and experimental evidence of filtering effect for surface Rayleigh waves at MHz frequencies in a structured block of marble 20 years ago [22], and some proposal for a decameter scale phononic crystal was formulated, although not substantiated by *in situ* experiments. Let us note that this seminal work which predates the birth of seismic metmaterials did not study the Rayleigh waves propagating in a soft substrate with air-holes, which is more relevant to the large scale experiments [2, 3].

It is also worthwhile mentioning the study on a meter scale phononic crystal [23] for airborne sound waves, by some of the authors of [22]. This PC is a sculpture sculpted by an artist Eusebio Sempere exhibited by the Juan March foundation in Madrid which consists of stainless-steel hollow cylinders 2.9 cm in diameter, with center to center spacing of 10 cm, fixed to a circular platform 4 m in diameter. This sculpture displays stop band properties between 1.5 and 4.5 kHz with good agreements between numerics and experiments. This famous sculpture is reminiscent of a forest of trees with graded height. Such graded forests have been revisited recently in the context of Rayleigh waves [24], based on some analogies with the rainbow effect in optics [25].

Localized resonant structures for elastic waves propagating within three-dimensional cubic arrays of thin coated spheres [26] and fluid filled Helmholtz resonators [27] paved the way towards acoustic analogues of the electromagnetic metamaterials [28] and [29], including elastic cloaks [30–32]. The control of elastic wave trajectories in thin plates was reported numerically [33, 34] and experimentally in 2012 [35] and extended to the realm of surface seismic waves in civil engineering applications in 2014 [2].

Building upon analogies between the physics of flexural waves in structured plates and the Rayleigh waves in structured soils to control surface seismic wave trajectories is not an incremental step. In order to achieve this goal, we had to solve conceptual and technological challenges. To name a few, the duraluminium plate used [20] is a homogeneous isotropic medium with simple geometric and elastic parameters, while the soil [2, 3] is heterogeneous and can only be ascribed some isotropic, homogeneous linear (e.g. non viscous) elastic parameters to certain extent, so its theoretical and numerical analysis requires some simplified assumption that can lead to inaccurate wave simulations. This means an experimental validation is absolutely necessary. Besides, Rayleigh waves are generated by anthropic sources such as an explosion or a tool impact or vibration (sledge-hammer, pile driving operations, vibrating machine footing, dynamic compaction, etc.), and this makes the numerical simulations even more challenging. Fortunately, an excellent agreement was noted between theory and experiment in [2], and this opens an unprecedented avenue in the design of large scale phononic crystals for the control of seismic waves, coined seismic metamaterials [3].

In 1968, R.D. Woods [36] created *in situ* tests with a 200–350 Hz source to show the effectiveness of isolating circular or linear empty trenches, with the same geometry, these results were compared in 1988 with numerical modeling studies provided by P.K. Banerjee [37].

The main thrust of this article is to point out the possibility to create seismic metamaterials not only for high frequency anthropic sources, but also for the earthquakes' typical frequency range i.e. from 0.1 to 12 Hz.

Let us now go back to the roots of the seismic metamaterials' design that counter intuitively rose from nanophotonics, with a typical frequency range in the terahertz, so at the very least one trillion times (10^{12}) higher than earthquakes.

3 Seismic megastructures

Let us first stress that the seismic megastructures we describe in this paper have metric to hectometric size. Basically, one can identify three main types of seismic metamaterials after a decade of research [38].

The first type includes structured soils made of cylindrical voids [2, 3, 39] or rigid inclusions [40, 41]. This group is called "Seismic Soil-Metamaterials" (SSM). The full-scale experiments with cylindrical holes described in [2] and [3] allowed the identification of the Bragg's effect similar to that in photonic crystals [2] and the distribution of energy inside the grid [3], which can be interpreted as the consequence of an effective negative refraction index (Figure 2). The flat seismic lens [3] is reminiscent of what Veselago and Pendry envisioned for light [6, 7].

The second group of seismic metamaterials consists of resonators buried in the soil in the spirit of tuned-mass dampers (TMD) like those placed atop of skyscrapers [42–44]. We call this group "buried mass-resonators" (BMR). This type of structured soil modifies the initial seismic signal applied at the base of the surface structure. In civil engineering word, it acts on the kinematic effect, which with the inertial effect, describes the soil-structure interaction [45].

The third type of seismic metamaterial consists of sets of above-surface resonators (ASR), including any type of rigid elements clamped in the ground, from trees

Figure 3: Medieval towers of Bologna.
Courtesy of The Time Machine by Genus Bononiae. Museum in the City (Bologna) and TOWER and POWER.

[24, 46, 47] to buildings [48]. It is specifically this type of structure that we present in this review paper (Figure 3).

Visionary research in the late 1980's based on the interaction of big cities with seismic signals and more recent studies on seismic metamaterials, made of holes or vertical inclusions in the soil, has generated interest in exploring the multiple interaction effects of seismic waves in the ground and the local resonances of both buried pillars and buildings.

Following the inspirational review article of Wegener's team at the Karlsruhe Institute for Technology [49], and ideas put forward by Housner [50, 51], Wirgin and Bard [52], Boutin [53], Philippe Guéguen [54] and his team at the Institute of Earth Science of Grenoble University observed that seismic noise could be modified in cities depending upon the specific arrangement and designs of tall buildings (Figure 3). Based on that idea, the concept of transformed metacities was launched in 2017 [48].

Interestingly, the idea of a dense urban habitat with high-rise buildings has already existed in the past. For instance, Figure 3 is a realistic reconstitution of the medieval city of Bologna with its tall towers. Some of them are still in place today with a height of almost 100 m.

4 Megastructures and soil-structure interaction

The metacity is a concept first put forward in the late 1980's on the basis of experimental observations of ground response and its devastating effects. It has been known, since the 1950's that the natural frequencies of any man-made structure are influenced by soil–structure interaction, especially on soft soils, and the presence of structures at the surface of a homogeneous half-space can significantly modify the ground motion [55–58]. Most of the time, the problem of ground response is disconnected from that of the resonant response of buildings or group of buildings.

On the basis of studies carried out on the interaction of cities with the seismic signal [50, 51, 59–61] and on the interaction of buildings with each other [62] (what could be viewed as a form of multiple scattering similar to that in PCs), some authors propose further extensions of this concept [43] based on analogies with electromagnetic and seismic metamaterials [40, 41]. This theoretical approach is consistent with studies of several authors on the influence of the trees of a forest on the surface waves [24, 46, 47].

For the rest of our discussion we considered the building as an elastic element embedded in the ground. During the seismic disturbance, it remains in the elastic domain (Figure 4). Most of the vibration energy affecting nearby

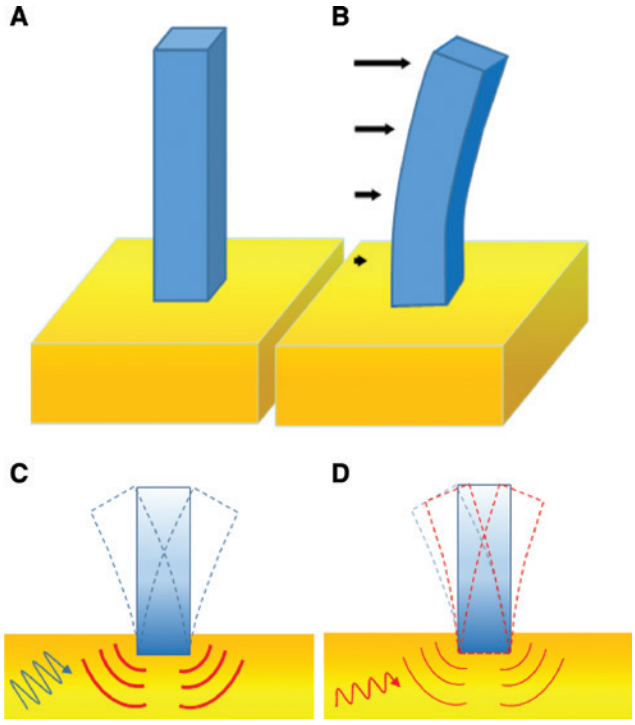

Figure 4: Deformation of building on a thick plate versus building under seismic disturbance: (A) Building at rest. (B) Elastic deformation for the first fundamental mode of the building. (C) Building under seismic disturbance and inertial interaction represented as a secondary seismic source, before the initial vibrational excitation. (D) Same as (C) after acting on the initial vibrational excitation. Acting on the input signal allows to influence, and particularly with the aim to decrease, the emitted vibration by the structure.

structures is carried by the Rayleigh surface waves. Earthquake engineering is concerned with the horizontal component of bulk and surface waves [2].

The response of a structure to an earthquake shake is affected by interactions between three linked systems: the structure, the foundation, and the soil underlying and surrounding the foundation. Soil-structure interaction analysis evaluates the collective response of these systems to a specified ground motion. The terms soil-structure interaction (SSI) and soil-foundation-structure interaction (SFSI) are both used to describe this effect [45].

The term free-field refers to motions that are not affected by structural vibrations or the scattering of waves at, and around, the foundation. SSI effects are absent for the theoretical condition of a rigid foundation supported on rigid soil.

We can summarize the objective of the design with the two schematics in Figure 4C and D. Under the initial seismic disturbance the structure generates a significant inertial effect at the soil-structure interface (C). The objective with seismic metamaterials is to reduce the amplitude and/or modify the frequency of the vibrational excitation in order to reduce the forces applied on the foundations and then, to improve their design (D). In both cases the inertial interaction could be described as a secondary seismic source emitted by the building itself. This is what we want to measure.

5 From transformation optics to transformation seismology

Actually, the field of transformational optics, which is 13 years old [63], can help explain metamaterial-like urbanism: when viewed from the sky, some modern cities and also older ones as in the medieval city of Bologna (Figure 3), look similar to invisibility cloaks.

Let us consider a mapping from a disc of radius $r = R_1$ onto an annulus $R_1 < r' < R_2$, known as Pendry's transform [63], as shown in Figure 5

$$r' = R_1 + r\frac{R_2 - R_1}{R_2} \tag{4}$$

This actually stretches the coordinate grid from Cartesian (left panel) to curvilinear (right panel) inside the annulus. This local deformation creates some effective anisotropy in the transformed medium in the optics case [63], and besides from that some chirality in the elasticity case [31, 32]. Chirality can be achieved to certain extent by the local torsion of buildings placed atop a soil (buildings behaving like spinning elements of so-called micropolar elasticity theory). Actually, due to the non-uniqueness of effective media describing a given composite, one can alternatively choose some Milton-Briane-Willis equations [30] to achieve the required chirality [64]. The required anisotropy can be achieved by a judicious placement of the buildings and groups of buildings, as shown in Figure 6.

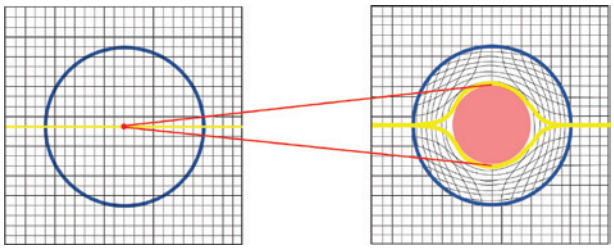

Figure 5: Illustration of the transformation of a disk into a ring (inspired by [63]).
The seismic ray in yellow passing through the center of the disk in the Cartesian coordinates (left) is detoured around the blown-up disk in the curvilinear coordinates (right). There is a direct analogy between ray trajectories in geometrical optics and seismology.

Figure 7 shows an elastodynamic wave simulation (in-plane fully coupled pressure and shear waves in soil) performed with the commercial finite element package

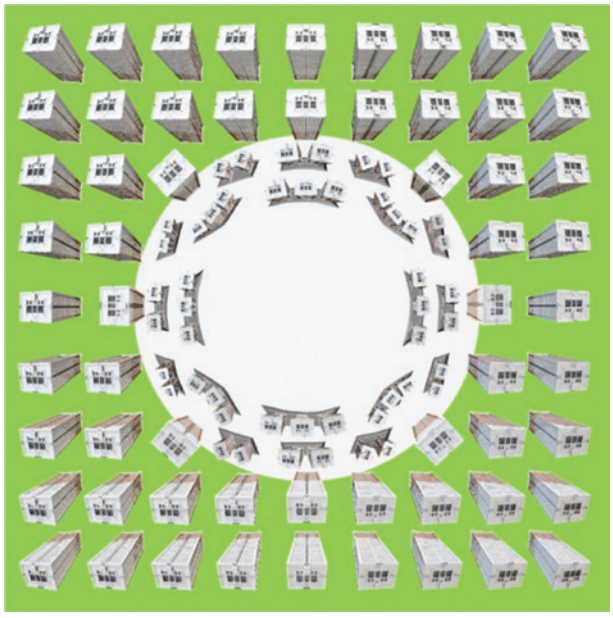

Figure 6: Top view of a megastructure made of a set of above-surface bending resonators (cf. Figure 4B).
Here each resonator is a tall building. The typical size of the seismic cloak is 1 km in diameter and the cloaked area (e.g. a park without any tall buildings, where civilians could seek some shelter and first aid e.g. with humanitarian organizations such as the Red Cross, Red Crescent and Red Crystal, and food supplies or any other convenience during an earthquake) is a disc in the center with a smaller diameter.

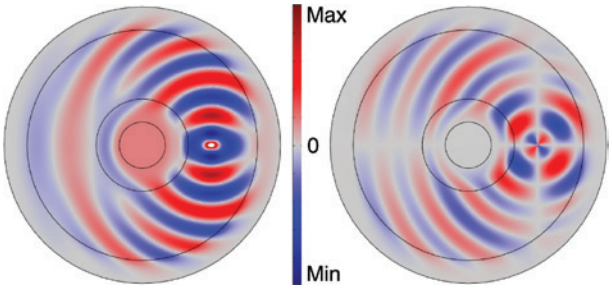

Figure 7: Numerical simulation (COMSOL MULTIPHYSICS) for a seismic source placed in close proximity of a seismic cloak (inner radius r_1 of 500 m and outer radius r_2 of 1000 m) with effective elastic parameters of soil and geometry compatible with the design in Figure 6. Medium surrounding the cloak is soft soil, source frequency is 0.1 Hz and polarization of the source is along the horizontal axis (compressional wave). The horizontal (dilatational) displacement (left) is not completely damped inside the inner disc (soil), but the vertical (shear) displacement (right) indeed vanishes. Such a cloak therefore offers protection against shearing (most deleterious wave polarization) and any large structure (i.e. an amphitheater or a stadium) placed in the center region would be safe.

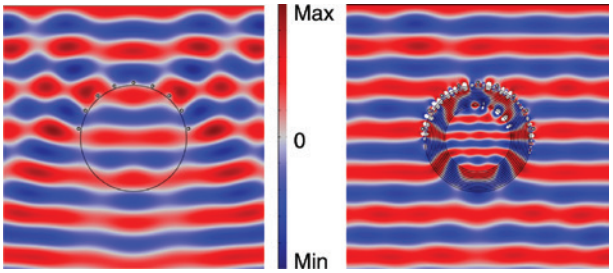

Figure 8: Numerical simulation (COMSOL MULTIPHYSICS) for a flexural plane wave propagating from top to bottom in a plate of thickness (15 m) small compared with the wavelength (800 m). (Left) Scattering by 9 regularly spaced clamped inclusions (of radius 6 m) along a semicircle of radius 1020 m. (Right) Same with a seismic cloak (inner radius r_1 of 500 m and outer radius r_2 of 1000 m) consisting of 10 layers of isotropic homogeneous layers with a negative Young's modulus and a negative density deduced from the same space folding transform as in [65, 66]. One notes the significantly reduced scattering in the right panel, as well as the exalted field on the cloak's outer boundary (cf. white spots where field magnitude is outside color scale, it is typically 3 times larger than elsewhere).

COMSOL MULTIPHYSICS. A source placed nearby a cloak with effective parameters similar to those in [31] i.e. with an anisotropic but also asymmetric elasticity tensor (the symmetry breaking being the hallmark of elastic chirality akin to magneto-optic activity), smoothly detours the pressure (left) and shear (right) wave polarizations around the disc in the center. However, one notes that the pressure component of the seismic wave does not vanish inside the disc. Fortunately, buildings are more resilient for pressure than shear vibrations, and the latter vanishes inside the disc, making it a safer zone to erect buildings. In terms of the megacity of Figure 6, one can say that the buildings within the annulus of the cloak and outside the cloak would be badly affected by the seismic wave, but the white region in the center (e.g. a park) would be a safe zone where people could gather and remain safe during an earthquake. One could also envisage building a large structure (e.g. an amphitheater or a stadium) in the white area, and provided its dimensions are different from those of the buildings constituting the cloak, it would be protected from the shear component of the earthquake.

6 Space folding transform for scattering cancellation of clamped inclusions

As noted in Figure 4B, a building can act as a secondary source, and thus can make an earthquake even more devastating as the combined effect of closely located building can create a strong seismic signal. One way to cancel the elastic signal of such seismic antennae is to implement the concept of external cloaking, see Figure 8, whereby negatively refracting isotropic elastic layers placed nearby nine clamped inclusions (such as concrete columns in soil clamped to a bedrock creating a zero frequency stop band in [40]), reduce dramatically the scattering of a plane (flexural) incident wave. The same holds true for stress-free inclusions, such as boreholes in soil, or for buildings placed atop a soil. In fact, the flat seismic lens in Figure 1 can be viewed as an external cloak as well, and thus suppression of scattering and vibrations from the building in Figure 2 could be attributed to a negatively refracting dynamic effective index associated with a space folding transform. It is interesting to note that proposal of external cloaking via anomalous resonances [67] of a core-shell system is rooted in a seminal paper published 25 years ago [68]. One notes the extreme enhancement of displacement field at the outer boundary of the external cloak in Figure 8, which could find potential application in energy harvesting.

Thus, we have essentially drawn some theoretical and numerical analogies between optics and elastodynamics, supported by two large scale experiments carried out in France in 2012 [2, 3]. We now focus on specific geophysics systems, and measurement techniques, in order to better bridge resonant phenomena for light in metamaterials with structured soil's vibrations in a seismically active region of the world.

7 Mexico-city: paradigm of soil-structure interaction and seismic ambient noise HVSR in megastructures

In this Section, the geophysical data are used only to show that the vibratory signature of some megastructures as skyscrapers could be identified in seismic noise acquisitions. We choose Mexico-city as this megalopolis of Latin-America is reminiscent of medieval towers of Bologna in Figure 3, and this exemplifies that site-city interactions such as the one shown in Figure 9 can occur in many megastructures worldwide throughout the centuries. We shall see in the sequel that some ancient structures are more resilient than megastructures such as Bologna in Europe and Mexico-city in South-America. We stress that other megastructures share similar features worldwide and also present a seismic hazard, to name a few New-York in North America, Istambul in in Middle-East, Lagos in Nigeria, Bombay in India, Shanghai in China and Sydney in Australia. The increase of megalopolises sizes presents a real challenge for seismic resilience, and so techniques to measure seismic hazard are of foremost important. Let us present the most popular one.

7.1 Principle of HVSR

Geological site conditions can generate significant changes in earthquake ground motion producing concentrated damage [70, 71]. It is usual to characterize the site effects by means of spectral ratios of recorded motions with respect to reference rock site [72]. These ratios are called empirical transfer functions and can be easily obtained for seismically active locations. It is often appropriate to interpret this transfer function assuming a 1-D soil configuration and deal with resonant frequencies and amplifications (Figure 10). Empirical transfer function could be compared to theoretical curves (Figure 11).

Initiated by Nakamura in 1989 [73] and widely studied to explain its strengths and limitations (seismological SESAME research project, [74–78]), the seismological microtremor horizontal-to-vertical spectral ratio (HVSR) method offers a reliable estimation of the soil resonance frequencies from the spectral ratio between horizontal and vertical motions of microtremors. This technique usually reveals the site dominant frequency f_0 but the amplitude of the HVSR is still not well understood [77].

The HVSR method was tested in geotechnical engineering too [78–80] by virtue of its ease of use. In restrictive conditions, as for homogeneous soil layer model with a sharp acoustic impedance contrast with the seismic substratum, the technique could be employed to estimate the

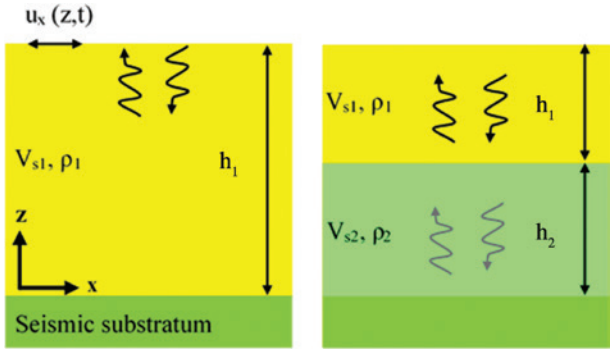

Figure 10: Schematics of wave propagation in a 1D soil-model. Homogeneous (left), two-layers model (right).

Figure 9: Evidence of soil-structure interaction in Mexico City (Photo courtesy of S. Brûlé and A.F.P.S. [69]).

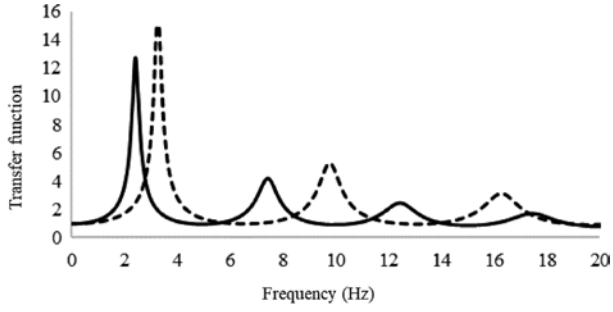

Figure 11: 1D soil-model.
Transfer function for the theoretical displacement at the seismic substratum and the free surface. The thickness of soil deposits is 20 m. The shear wave velocity V_s is 200 m.s^{-1} (black solid line) and 260 m.s^{-1} (black dotted line). The damping ratio is respectively 0.05 and 0.04.

ground fundamental frequency f_0. In this paper, we used this technique to point out both the fundamental low frequency of the alluvial basin and the frequencies of the LatinoAmericana Tower in Mexico city.

7.2 Geology of Mexico

The subsoil of the Mexico valley is known worldwide for its lacustrine clays (high water content) and its seismic site effects, especially after the dramatic major earthquake of September 19th, 1985 which led to more detailed studies [81]. Typically, the geotechnical zonation of Mexico city is made up of three areas: hills, transition, and ancient lake zone. The LatinoAmericana Tower is located on the lake bed zone where the thickness of clay exceeds 30 m (Figures 12 and 13). At the western part of the valley, the thickness of lacustrine deposits could reach 60 m. Shear wave velocity Vs for the clays typically presents very low values (lower than 100 m/s).

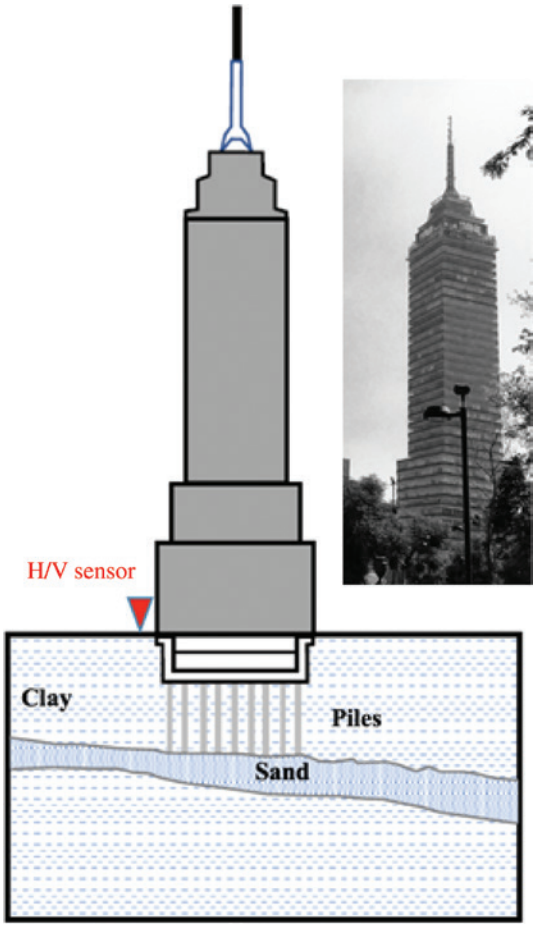

Figure 12: Schematic of Torre LatinoAmericana (182 m) and its deep pile-foundations.
The soil consists of clay, with a layer of sand, with an overall thickness over 30 m. The location of the velocimeter, whose specifications are given in Table 1, is indicated by the arrow. Photography courtesy of S. Brûlé.

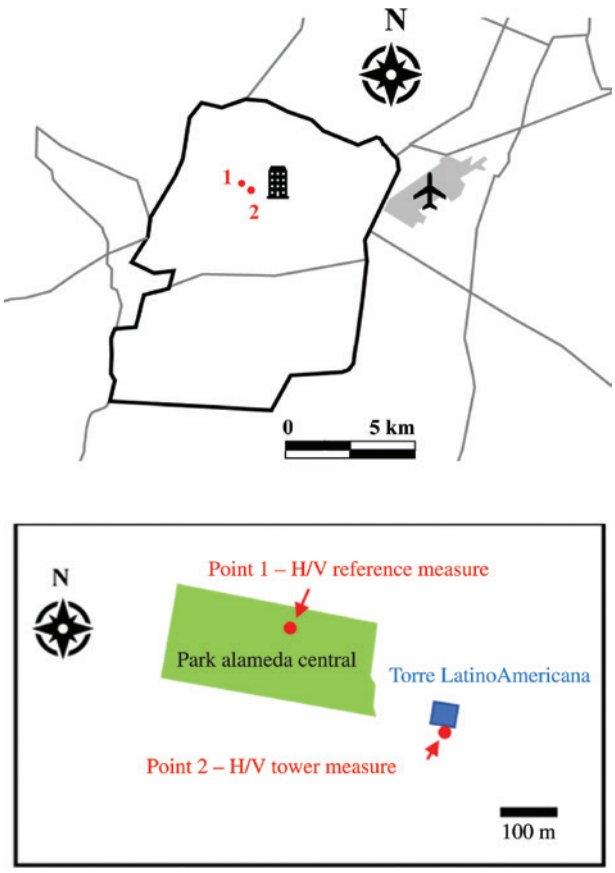

Figure 13: Schematic map of Mexico City Center and location of HVSR measures (1: reference measure; 2: tower measure), see also Table 2. Horizontal West-East distance separating 1 and 2 is 415 m.

7.3 Torre LatinoAmericana

Inaugurated in 1956, The LatinoAmericana Tower (Figure 12) is a 182 m high skyscraper with 44 floors. The square base is 34.4 × 34.4 m and the overall weigth of the tower is around 23,500 tons.

Its design consists of a steel-frame construction (H columns) and 361 deep-seated piles anchored at –33 m below the street level, in a little thick sand layer (5 m).

Considered as the most resistant (or one of the most resistant) building of Mexico city, it survived three destructive earthquakes: 1957/07/28 (moment magnitude M_w: 7.7), 1985/09/19 (moment magnitude M_w: 8.0) and 2017/09/19 (Magnitude M_w: 7.1). We can thus confer to this structure the merit for the tallest building ever exposed to huge seismic forces.

The ground surface subsidence problem of Mexico city necessitated a 13 m deep basement to reduce the net bearing pressure on the piles raft. The foundation is a rigid mat supported by piles [82] and [83]. The estimation of the different modes of vibration of the building gives 3.5–3.7 s for the fundamental, 1.5, 0.9, and 0.7 s for the harmonics [82]. The ground period for an earthquake is estimated between 1.5 and 2.5 s in the downtown which is located in the ancient lake area. Basically, an excitation of the second mode of the building is expected during an earthquake.

7.4 HVSR Measures

We chose two special locations for the HVSR measures with the aim to have the same soil fundamental frequency f_0 on both graphs and to point out the characteristic frequency of the tower vibration. For that, the reference measure was recorded in the central part of a plant park with no buildings within 200 m of distance, see Figure 13. The measure for the building was taken outside at 1 m from the building wall of the ground floor, on a concrete slab, as indicated by the arrow on Figure 12. Each measure was double-recorded with two independent sensors. The horizontal distance between the two spots is 415 m.

The present study used a highly portable (10×14×7.7 cm (height), 1.1 kg) three component (2 horizontal and 1 vertical directions) high-resolution electrodynamic sensor (Tromino™ from Micromed) for the measurement of the ambient vibrations at the observation point or station. The technical characteristics of the sensor are given in Table 1.

The HVSR measurements in this study were made in compliance with the guidelines of SESAME [84], so the step-by-step methodology will not be repeated here except to highlight a few salient points. Before taking the measurement, the sensor was aligned and firmly secured to the ground by a set of spikes. Seismic noise was recorded with a sampling rate of 512 Hz for 30 min at each site, this is to ensure that there is adequate statistical sampling in the range 0.1–100 Hz, the frequency range of engineering interest.

Table 1: Digital velocimeter specifications.

Velocimeter specifications	
Frequency response	0.1–256 Hz
Dynamic range	180 Db
Sample rate per channel	32 kHz
Output sampling rate	128, 256 or 512 Hz

The HVSR curves were calculated by averaging the H/V (horizontal-vertical) ratios obtained after dividing the signal into non-overlapping 20-s windows (which is sufficient for the spectra above 1 Hz). Each window was detrended, tapered, padded, FF-transformed and smoothed with triangular windows of width equal to 10% of the central frequency.

The ratio of the H/V Fourier amplitude spectra is expressed with Eq. (5), where $F_V(\omega)$ and $F_H(\omega)$ denote the vertical and horizontal Fourier amplitude spectra, respectively.

$$\mathrm{HVSR}(\omega) = \frac{|F_H(\omega)|}{|F_V(\omega)|} \tag{5}$$

The geometric average was used to combine EW and NS components in the single horizontal (H) spectrum, and then it was divided by the vertical component (V) to produce the measured HVSR curve as shown in Eq. (6).

$$\mathrm{HVSR}_m = \frac{\sqrt{H_{EW} \times H_{NS}}}{V} \tag{6}$$

Furthermore, the stability of the HVSR curves was verified and used to identify the presence of artifacts from anthropic noise (machinery, industrial areas, etc.).

8 Results and discussions

Results are presented in Figure 14, and Table 3.

In the frequency range of engineering interest, it can be noted first that a clear distinctive peak appears for all the measures and the amplification is five times, at least.

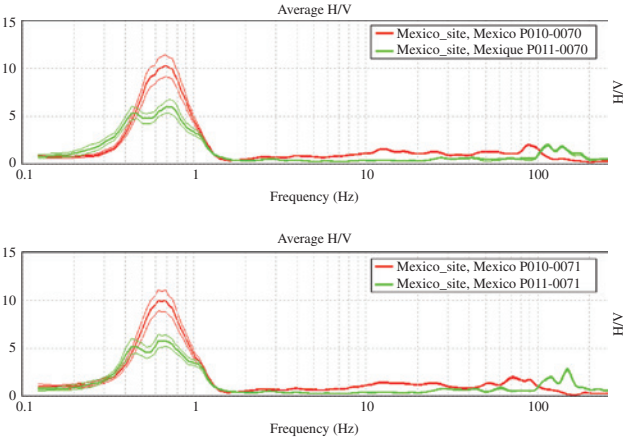

Figure 14: HVSR results.
Measure 1 and 2 in same graph for sensor 70 (Top) and for sensor 71 (Bottom).

Table 2: Location of the HVSR measures.

Spot	Latitude	Longitude	City	Location
1	19,4361	−99,1436	Mexico	Alameda Central
2	19,4337	−99,1406	Mexico	Torre Latino Americana

Table 3: HVSR results.

Spot	Sensor	First dominant frequency Hz	T at dominant frequency s	Second dominant frequency Hz	T at dominant frequency s
1	70	0.69±0.11	1.45		
1	71	0.63±0.11	1.59		
2	70	0.72±0.11	1.39	~0.45	2.22
2	71	0.69±0.11	1.45	~0.42	2.38

Fine line curves represent the 95% of interval of confidence. These curves are very close to the average solid red or green curve, indicating a good quality of measurement.

For the point 1 in the park, the average period (sensors 70 and 71) at the dominant frequency is 1.52 s. For the point 2, close to the tower, this average period is 1.42 s. We remind that a horizontal distance of 415 m separates the two points. The overall geology of the basin is known to be stable between these two points, but local variations may exist.

For the measure 2, a second frequency peak at 0.45 Hz (sensor 70) and 0.42 Hz (sensor 71) is observed in Figure 14. The mean period is 2.3 s, this period around 2 s could be the signature of the vibration generated by the tower itself on its close environment. We do not distinguish the fundamental period of the tower (3.5–3.7 s) nor its harmonics (1.5, 0.9, and 0.7 s). However, it should also be kept in mind that many earthquakes experienced by a structure may have changed the values of the initial modes as well as the ground-foundation-structure interface conditions.

Frequencies peak above 10 Hz could be attributed to a forest of trees in the park, as these present similarity with filtering effects observed and numerically justified for a forest of trees in Grenoble [24].

9 Conclusions and perspectives

We have seen that seismic metamaterials is rooted in research advances in nanophotonics. The radical change of scale from nanometers to decameters suggests that many analogies drawn between light and seismic wave phenomena break down, but large scale experiments come to our rescue and backup the bold claim of negative refraction, lensing, and cloaking taking place in soft soils structured at the decameter scale. While working on this review article, we realized that there are striking similarities between an invisibility cloak tested for various types of waves [85] and sky views of antique Gallo-Roman theaters [86–88], see Figure 15.

It seems to us that such architectures are more resilient, thanks to their unique design. Perhaps this is the reason why some of these megastructures, such as amphitheaters have remained mostly intact through the centuries. This deserves to be studied in more detail, and we hope our preliminary observations will foster efforts in the search for more analogies between engineered electromagnetic metamaterials and a new type of seismic metamaterials which we propose to call “archeological metamaterials”.

Another interesting aspects of seismic metamaterials which we would like to further investigate is the extreme

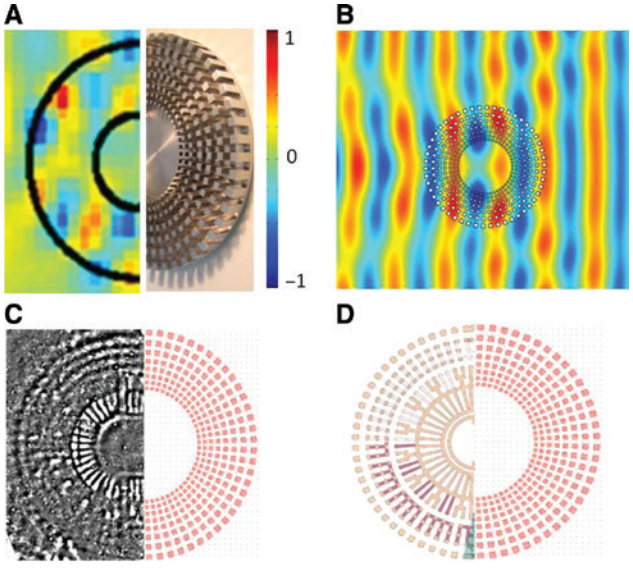

Figure 15: Analogy between an invisibility cloak and antique Gallo-Roman theaters: (A) Electric field from microwave experiment at 3.5 GHz (courtesy of R. Abdeddaim and E. Georget) and photo (CNRS/INSIS/Institut Fresnel) of an aluminium cloak 20 cm in diameter. (B) Numerical simulation (COMSOL MULTIPHYSICS) of a plane flexural incident from the left at 5 Hz on multiply perforated cloak [34] with inner radius r_1 of 50 m and outer radius r_2 of 100 m, in a 5 m thick plate consisting of clay (real part of out-of-plane displacement field is shown). (C) Photo montage of a sky geophysics view extracted from a magnetic gradient map of a completely buried Gallo-Roman ex muros theater located at Autun, La Genetoye (France) versus the cloak (courtesy of Geocarta and G. Bossuet, in [86] with the permission of the authors). (D) Same comparison with a part of the foundations of the antique theater (courtesy of A. Louis (PCR) and Hydrogeotechnique [87]).

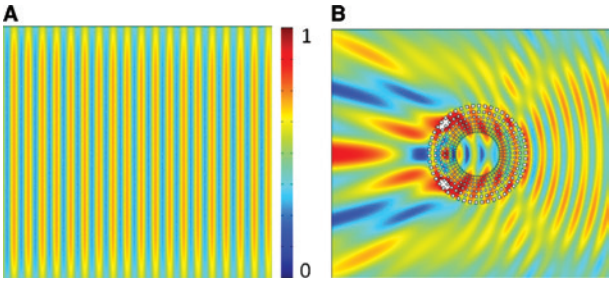

Figure 16: Numerical simulations (COMSOL MULTIPHYSICS) of a flexural plane wave propagating at 5 Hz in a 5 m thick homogeneous plate of clay (A) and same (B) with a distribution of boreholes as in Figure 15B. Magnitude of out-of-plane displacement field (normalized with respect to source) is shown and its enhancement in the corridors of the cloak should be noted. The two white spots in (B) correspond to maxima of field magnitude in the range [1, 1.5] outside the color scale.

field inside the structured cloak in Figure 15B, which is more apparent in Figure 16. This large field enhancement can be attributed to the fast oscillating field in the interstitial space (soil) between the perforations (the smaller the interstitial space, the faster the oscillations and thus larger the gradient of the field therein): this can be viewed as a network of close-to-touching stress-free walls trapping flexural waves for which a similar phenomenon occurs in photonics [69]. As an indirect consequence, this finding could be particularly important in the perspective of converting such mechanical energy that is continually exalted by the continuous seismic noise in these corridors that we call "energy seismic corridors". These theoretical buried structures trapping seismic ambient noise could be specifically designed for the unique purpose of electrical energy supply, for instance.

We realize one might argue that soil is inherently viscous and thus the large field enhancement in these energy seismic corridors might be counteracted by dissipation. But here again, some interesting parallels can be drawn with nanoplasmonics, where some problems of dissipation of light propagating at metal surface structured with close to touching boreholes at the nanometer scale [89, 90], have been addressed by adding some gain, and this could inspire future research in energy seismic corridors. Such issues of dissipation and gain naturally lead to the fascinating topic of Parity-Time symmetry in photonics. A recent work suggests non-linearity might counteract dissipation in photonics [91]. Non-reciprocity and topology [92, 93] is another vibrant topic in photonics that could inspire improved designs of seismic cloaks that would support states of surface waves immune to back scatter and robust against imperfections caused by soil heterogenity and construction work. Due to permanent and free seismic ambient noise, we believe energy seismic corridors in a large scale seismic cloak might also be a valuable way to harness seismic energy independently of the cloaking role for major earthquake of the buried megastructure.

Finally, the future of seismic metamaterials might be brighter if physicists and civil engineers, not only draw useful analogies with design of electromagnetic metamaterials and metasurfaces, but also take a closer look at ancient architectures and learn from these beautiful and amazingly resilient designs.

Acknowledgements: S.G. would like to acknowledge the group of Prof. R.V. Craster at Imperial College London for a visiting position. S.B. especially thanks Association Française de Génie Parasismique (A.F.P.S.) [94] that has organized the Mexico mission in 2017, C. Boutin, S. Hans and T. Doanh from Ecole Nationale des Travaux Publics de l'Etat at Vaulx en Velin, France for funding him H/V sensors. S.B. would like to acknowledge all the authors involved in PCR Project [88] for the archeological materials and permissions for figures, and would like to thank Y. Labaune (Director of "Service Archéologique de la Ville d'Autun, France"), A. Louis (Direction de l'Aménagement, Service de l'Archéologie, Conseil Départemental d'Eure-et-Loir, Chartres, France), J-B and J-C Gress (Direction of Hydrogéotechnique), H. Grisey (Technical Direction at Hydrogéotechnique), L. Colin (Université de Franche-Comté and Director of the subsidiary of Hydrogéotechnique at Belfort) and F. Ferreira (Director of archeological excavation at La Genetoye, Autun), more personally.

References

[1] Gaponenko SV. Introduction to nanophotonics, 1st ed., Cambridge University Press, Cambridge, 2010.
[2] Brûlé S, Javelaud EH, Enoch S, Guenneau S. Experiments on seismic metamaterials: molding surface waves. Phys Rev Lett 2014;112:133901.
[3] Brûlé S, Javelaud EH, Enoch S, Guenneau S. Flat lens for seismic waves. Sci Rep 2017;7:18066.
[4] Yablonovitch E. Inhibited spontaneous emission in solid-state physics and electronics. Phys Rev Lett 1987;58:2059–62.
[5] John S. Strong localization of photons in certain disordered dielectric superlattices. Phys Rev Lett 1987;58:2486–9.
[6] Veselago VG. The electrodnamics of substances with simultaneously negative values of ε and μ. Sov Phys Usp 1968;10:509–14.
[7] Pendry JB. Negative refraction makes a perfect lens. Phys Rev Lett 2000;85:3966–9.
[8] Srinivasan K, Painter O. Momentum space design of high-q photonic crystal optical cavities. Opt Express 2002;10:670–84.
[9] Zengerle R. Light propagation in singly and doubly periodic waveguides. J Mod Opt 1987;34:1589–617.

[10] Notomi M. Theory of light propagation in strongly modulated photonic crystals: refractionlike behaviour in the vicinity of the photonic band gap. Phys Rev B 2000;62:10696–705.
[11] Gralak B, Enoch S, Tayeb G. Anomalous refractive properties of photonic crystals. J Opt Soc Am A 2000;17:1012–20.
[12] Luo C, Johnson SG, Joannopoulos JD, Pendry JB. All angle negative refraction without negative effective index. Phys Rev B 2002;65:201104.
[13] Pendry JB, Holden AJ, Robbins DJ, Stewart WJ. Magnetism from conductors and enhanced nonlinear phenomena. IEEE Trans Microw Theory Tech 1999;47:2075–84.
[14] Smith DR, Padilla WJ, Vier VC, Nemat Nasser SC, Schultz S. Composite medium with simultaneously negative permeability and permittivity. Phys Rev Lett 2000;84:4184.
[15] Dolling G, Enkrich C, Wegener M, Soukoulis CM, Linden S. Observation of simultaneous negative phase and group velocity of light. Science 2006;312:892–4.
[16] Schurig D, Mock JJ, Justice BJ, et al. Metamaterial electromagnetic cloak at microwave frequencies. Science 2006;314:977–80.
[17] Alù A, Silveirinha M, Salandrino A, Engheta EN. Epsilon near-zero metamaterials and electromagnetic sources: tailoring the radiation phase pattern. Phys Rev B 2007;75:155410.
[18] Enoch S, Tayeb G, Sabouroux P, Guérin N, Vincent P. A metamaterial for directive emission. Phys Rev Lett 2002;89:213902.
[19] Antonakakis T, Craster RV. High frequency asymptotics for microstructured thin elastic plates and platonics. Proc R Soc Lond A 2012;468:1408–27.
[20] Dubois M, Bossy E, Enoch S, Guenneau S, Lerosey G, Sebbah P. Time drive super oscillations with negative refraction. Phys Rev Lett 2015;114:013902.
[21] Sukhovich A, Merheb B, Muralidharan K, et al. Experimental and theoretical evidence for subwavelength imaging in phononic crystals. Phys Rev Lett 2009;102:154301.
[22] Meseguer F, Holgado M, Caballero D, et al. Rayleigh-wave attenuation by a semi-infinite two-dimensional elastic-band-gap crystal. Phys Rev B 1999;59:12169.
[23] Martinez-Sala R, Sancho J, Sanchez JV, Gomez V, Llinares J, Meseguer F. Sound attenuation by sculpture. Nature 1995;378:241.
[24] Colombi A, Roux P, Guenneau S, Guéguen P, Craster RV. Forests as a natural seismic metamaterial: rayleigh wave bandgaps induced by local resonances. Sci Rep 2016;6:19238.
[25] Tsakmakidis KL, Boardman AD, Hess O. Trapped rainbow storage of light in metamaterials. Nature 2007;450:397.
[26] Liu Z, Zhang X, Mao Y, et al. Locally resonant sonic materials. Science 2000;289:1734–6.
[27] Fang N, Xi D, Xu J, et al. Ultrasonic metamaterials with negative modulus. Nat Mater 2006;5:452–6.
[28] Christensen J, Garcia De Abajo FJ. Anisotropic metamaterials for full control of acoustic waves. Phys Rev Lett 2012;108:124301.
[29] Craster R, Guenneau S. Acoustic metamaterials: negative refraction, imaging, lensing and cloaking. In: Craster R, Guenneau S, eds. Vol. 166, Springer Verlag, 2013.
[30] Milton GW, Briane M, Willis JR. On cloaking for elasticity and physical equations with a transformation invariant form. New J Phys 2006;8:248.
[31] Brun M, Guenneau S, Movchan AB. Achieving control of in-plane elastic waves. Appl Phys Lett 2009;94:061903.
[32] Norris A, Shuvalov AL. Elastic cloaking theory. Wave Motion 2011;48:525–38.
[33] Farhat M, Guenneau S, Enoch S. Ultrabroadband elastic cloaking in thin plates. Phys Rev Lett 2009;103:024301.
[34] Farhat M, Guenneau S, Enoch S. Broadband cloaking of bending waves via homogenization of multiply perforated radially symmetric and isotropic thin elastic plates. Phys Rev B 2012;85:020301 R.
[35] Stenger N, Wilhelm M, Wegener M. Experiments on elastic cloaking in thin plates. Phys Rev Lett 2012;108:014301.
[36] Woods RD. Screening of surface waves in soils, Technical Report No. IP-804. University of Michigan, 1968.
[37] Banerjee PK, Ahmad S, Chen K. Advanced application of BEM to wave barriers in multi-layered three-dimensional soil media. Earthq Eng Struct Dynam 1988;16:1041–1060.
[38] Brûlé S, Enoch S, Guenneau S. Emergence of seismic metamaterials: current state and future perspectives. arXiv:1712.09115, 2017.
[39] Brûlé S, Javelaud E, Guenneau S, Enoch S, Komatitsch D. Seismic metamaterials. Proceedings of the 9th International Conference of the Association for Electrical, Transport and Optical Properties of Inhomogeneous Media in Marseille, France, 2012.
[40] Achaoui Y, Antonakakis T, Brûlé S, Craster RV, Enoch S, Guenneau S. Clamped seismic metamaterials: ultra-low broad frequency stop-bands. New J Phys 2017;19:063022.
[41] Aznavourian R, Puvirajesinghe T, Brûlé S, Enoch S, Guenneau S. Spanning the scales of mechanical metamaterials using time domain simulations in transformed crystals, graphene flakes and structured soils. J Phys: Condens Matter 2017;29:433004.
[42] Krödel S, Thome N, Daraio C. Wide band-gap seismic metastructures. Ex Mech Lett 2015;4:111–7.
[43] Achaoui Y, Ungureanu B, Enoch S, Brûlé S, Guenneau S. Seismic waves damping with arrays of inertial resonators. Ex Mech Lett 2016;8:30–8.
[44] Finocchio G, Casablanca O, Ricciardi G, et al. Seismic metamaterials based on isochronous mechanical oscillators. Appl Phys Lett 2014;104:191903.
[45] Brûlé S, Cuira F. Practice of soil-structure interaction under seismic loading. AFNOR Edition, 2018.
[46] Colombi A, Colquitt D, Roux P, Guenneau S, Craster RV. A seismic metamaterial: the resonant metawedge. Sci Rep 2016;6:27717.
[47] Maurel A, Marigo JJ, Pham K, Guenneau S. Conversion of Love waves in a forest of trees. Phys Rev B 2018;98:134311.
[48] Brûlé S, Ungureanu B, Achaoui Y, et al. Metamaterial-like transformed Urbanism. Innov Infrastruct Solut 2017;2:20.
[49] Kadic M, Bückmann T, Schittny R, Wegener M. Metamaterials beyond electromagnetism. Rep Prog Phys 2013;76:126501.
[50] Housner GW. Effect of foundation compliance on earthquake stresses in multistory buildings. Bull Seismol Soc Am 1954;44:551–69.
[51] Housner GW. Interaction of building and ground during an earthquake. Bull Seismol Soc Am 1957;47:179–86.
[52] Wirgin A, Bard P-Y. Effects of buildings on the duration and amplitude of ground motion in Mexico City. Bull Seismol Soc Am 1996;86:914–20.
[53] Boutin C, Roussillon P. Assessment of the urbanization effect on seismic response. Bull Seismol Soc Am 2004;94:251–68.
[54] Guéguen P, Bard P-Y, Chavez-Garcia FJ. Site-city seismic interaction in Mexico City-like environments: an analytical study. Bull Seismol Soc Am 2002;92:794–811.

[55] Clouteau D, Aubry D. Modification of the ground motion in dense urban areas. J Comput Acoust 2011;9:1659–75.
[56] Guéguen P, Bard P-Y, Semblat J-F. From soil-structure interaction to site-city interaction. In: 12th World Conference on Earthquake Engineering. Auckland, New Zealand, 2000.
[57] Trifunac MD. Interaction of a shear wall with the soil for incident plane SH waves. Bull Seismol Soc Am 1972;62: 63–83.
[58] Wong HL, Trifunac MD, Westermo B. Effects of surface and subsurface irregularities on the amplitude of monochromatic waves. Bull Seismol Soc Am 1977;67:353–68.
[59] Auriault JL, Boutin C, Geindreau C. Homogénéisation de phénomènes couplés en milieux hétérogènes, Mécanique et Ingéniérie des Matériaux, Hermes, Lavoisier, 2009.
[60] Boutin C, Roussillon P. Wave propagation in presence of oscillators on the free surface. Int J Eng Sci 2006;4:180–204.
[61] Ghergu M, Ionescu IR. Structure–soil–structure coupling in seismic excitation and city effect. Int J Eng Sci 2009;47:342–54.
[62] Spiliopoulos KV, Anagnospoulos SA. Earthquake induced pounding in adjacent building. In: Earthquake engineering, 10th World Conference, Balkema, Rotterdam, 1992.
[63] Pendry JB, Schurig D, Smith DR. Controlling electromagnetic fields. Science 2006;312:1780–2.
[64] Kadic M, Diatta A, Frenzel T, Guenneau S, Wegener M. Static chiral Willis continuum mechanics for three-dimensional chiral mechanical metamaterials. Phys Rev B 2019;99:214101.
[65] Liu Y, Gralak B, McPhedran RC, Guenneau S. Finite frequency external cloaking with complementary bianisotropic media. Opt Express 2014;22:17387–402.
[66] Abdeddaim R, Enoch S, Guenneau S, McPhedran RC. Experiments on external cloaking: electromagnetic space (in submission).
[67] Milton GW, Nicorovici NA. On the cloaking effects associated with anomalous localized resonance. Proc R Soc A 2006;462:3027–59.
[68] Nicorovici NA, McPhedran RC, Milton GW. Optical and dielectric properties of partially resonant composites. Phys Rev B 1994;49:8479–82.
[69] AFPS, Report of the post-seismic mission on the Mexico earthquake of september 19th, 2017. AFPS, 2018.
[70] Sánchez-Sesma FJ. Site effects on strong ground motion. Soil Dyn Earthq Eng 1987;6:124–32.
[71] Aki K. Local site effects on strong ground motion, in Earthquake Engineering and Soil Dynamics I –Recent Advances in Ground Motion Evaluation, In: Von Thun JL, ed. Geotech. Special Pub. No. 20, ASCE, New York, NY, 1988, 103–55.
[72] Cadet H, Bard P-Y, Rodriguez-Marek A. Defining a standard rock site: propositions based on the KiK-net database. Bull Seism Soc Am 2010;100:172–95.
[73] Nakamura Y. A method for dynamic characteristics estimation of subsurface using microtremor on the ground surface. Q Rep Railw Tech Res Inst 1989;30:25–30.
[74] Bonnefoy-Claudet S, Cornou C, Bard P-Y, et al. H/V ratio: a tool for site effects evaluation. Results from 1-D noise simulations. Geophys J Int 2006;167:827–37.
[75] Bard P-Y. The H/V technique: capabilities and limitations based on the results of the SESAME project. Foreword. Bull Earthq Eng 2008;6:1–2.
[76] Pilz M, Parolai S, Leyton F, Campos J, Zschau J. A comparison of site response techniques using earthquake data and ambient seismic noise analysis in the large urban areas of Santiago de Chile. Geophys J Int 2009;178:713–28.
[77] Lunedei E, Albarello D. Theoretical HVSR curves from full wavefield modelling of ambient vibrations in a weakly dissipative layered Earth. Geophys J Int 2010;181:1093–108.
[78] Brûlé S, Javelaud EH, Ohmachi T, Nakamura Y, Inoue S. H/V method used to qualify the modification of dynamic soil characteristics due to ground improvement work by means of heavy compaction process. A case study: the former Givors's glass factory area", 7th International Conference on Urban Earthquake Engineering and 5th International Conference on Earthquake Engineering, Tokyo, Japan, 02-26, 2010, 451–5.
[79] Brûlé S, Javelaud E. Méthode H/V en géotechnique. Application à un modèle bicouche. Rev Fr Géotech N 2014;142:3–15.
[80] Harutoonian P, Leo CJ, Doanh T, et al. Microtremor measurements of rolling compacted ground. Soil Dyn Earthq Eng 2012;4:23–31.
[81] Auvinet G, Méndez E, Juárez M. The subsoil of Mexico City. Vol. III. Three volumes edition celebrating the 60th Anniversary of The Institute of Engineering, UNAM, 2017.
[82] Zeevaert L. Foundation design and behaviour of Tower Latino American in Mexico City. Géotechnique 1957;7:115–33.
[83] Boorman R, Tomlinson MJ. Foundation design and construction. Published by Longman Group United Kingdom, 2001.
[84] SESAME, Guidelines for the implementation of the H/V spectral ratio technique on ambient vibrations – measurements, processing and interpretations. SESAME European research project. deliverable D23.12, 2005.
[85] Xu J, Jiang X, Fang N, et al. Molding acoustic, electromagnetic and water waves with a single cloak. Sci Rep 2015;5:10678.
[86] Bossuet G, Louis A, Ferreira F, Labaune Y, Laplaige C. Le sanctuaire suburbain de la Genetoye à Autun/Augustodunum (Saône-et-Loire). Apport de l'approche combinée de données spatialisées à la restitution du théâtre antique du Haut du Verger, Gallia, 72-2, 2015, 205–23.
[87] SolscopeMag, Quelles fondations pour le théâtre antique de la Plaine de l'Arroux, à Autun ? 2016;6:81–4.
[88] Alix S, Barral P, Ducreux F, et al. Projet collectif de recherche, Approches diachroniques et pluridisciplinaires de la confluence Arroux / Ternin de la préhistoire au Moyen-âge. Le complexe monumental de la Genetoye (Autun, Saône-et-Loire) dans son environnement, rapport PCR, 2018, 84.
[89] Movchan AB, Movchan NV, Guenneau S, McPhedran RC. Asymptotic estimates for localized electromagnetic modes in doubly periodic structures with defects. Proc Roy Soc Lond. A 2007;463:1045–67.
[90] Hess O, Pendry JB, Maier SA, Oulton RF, Hamm JM, Tsakmakidis KL. Active nanoplasmonic metamaterials. Nat Mater 2012;11:573–84.
[91] Williams CR, Andrews SR, Maier SA, Fernandez-Domínguez AI, Martín-Moreno L, García-Vidal FJ. Highly confined guiding of terahertz surface plasmon polaritons on structured metal surfaces. Nat Photonics 2008;2:175–9.
[92] Miri MA, Alù A. Nonlinearity-induced PT-symmetry without material gain. New J Phys 2016;18:065001.
[93] Khanikaev AB, Shvets G. Two-dimensional topological photonics. Nat Photonics 2017;11:763–73.
[94] Makwana MP, Craster RV. Designing multidirectional energy splitters and topological valley supernetworks. Phys Rev B 2018;98:235125.